

Higgs-boson and Z-boson flavor-changing neutral-current decays correlated with B-meson decays in the littlest Higgs model with T parity

Xiao-Fang Han, Lei Wang, and Jin Min Yang

Institute of Theoretical Physics, Academia Sinica, Beijing 100190, China

(Received 31 July 2008; published 20 October 2008)

In the littlest Higgs model with T -parity new flavor-changing interactions between mirror fermions and the standard model (SM) fermions can induce various flavor-changing neutral-current decays for B -mesons, the Z -boson, and the Higgs boson. Since all these decays induced in the littlest Higgs with T -parity model are correlated, in this work we perform a collective study for these decays, namely, the Z -boson decay $Z \rightarrow b\bar{s}$, the Higgs-boson decay $h \rightarrow b\bar{s}$, and the B -meson decays $B \rightarrow X_s \gamma$, $B_s \rightarrow \mu^+ \mu^-$, and $B \rightarrow X_s \mu^+ \mu^-$. We find that under the current experimental constraints from the B -decays, the branching ratios of both $Z \rightarrow b\bar{s}$ and $h \rightarrow b\bar{s}$ can still deviate from the SM predictions significantly. In the parameter space allowed by the B -decays, the branching ratio of $Z \rightarrow b\bar{s}$ can be enhanced up to 10^{-7} (about one order above the SM prediction) while $h \rightarrow b\bar{s}$ can be much suppressed relative to the SM prediction (about one order below the SM prediction).

DOI: [10.1103/PhysRevD.78.075017](https://doi.org/10.1103/PhysRevD.78.075017)

PACS numbers: 14.80.Cp, 11.30.Qc, 12.60.Fr

I. INTRODUCTION

The fancy idea of little Higgs [1] tries to provide an elegant solution to the hierarchy problem by regarding the Higgs boson as a pseudo-Goldstone boson whose mass is protected by an approximate global symmetry and free from one-loop quadratic sensitivity to the cutoff scale. The littlest Higgs model [2] is a cute economical implementation of the little Higgs idea, but is found to be subject to strong constraints from electroweak precision tests [3], which would require raising the mass scale of the new particles to far above TeV scale and thus reintroduce the fine-tuning in the Higgs potential [4]. To tackle this problem, a discrete symmetry called T -parity is proposed [5], which forbids the tree-level contributions from the heavy gauge bosons to the observables involving only standard model (SM) particles as external states. However, in the littlest Higgs model with T -parity (LHT) [5], there are new flavor-changing interactions between mirror fermions and the SM fermions (just like the flavor-changing interactions between sfermions and fermions in supersymmetric models). Such new flavor-changing interactions can induce various flavor-changing neutral-current (FCNC) processes, which should be examined.

Among various FCNC processes induced by the new flavor-violating interactions in the LHT model, the loop-induced B -decays, such as $B \rightarrow X_s \gamma$, $B_s \rightarrow \mu^+ \mu^-$, and $B \rightarrow X_s \mu^+ \mu^-$, should be first checked due to the available experimental data on these decays. Recently, these B -decays have been intensively examined in the LHT model, which were found to be sensitive to the new flavor-violating interactions [6–9]. Note that in addition to these B -decays, the loop-induced FCNC decays of the Higgs and Z -boson, such as $Z \rightarrow b\bar{s}$ and $h \rightarrow b\bar{s}$ which are strongly correlated with the FCNC B -decays, should also be examined since they are sensitive to the flavor structure

of new physics. In the future there may be at least two avenues in which Z -bosons will be produced in much larger quantities than at LEP. At the CERN Large Hadron Collider (LHC) with an integrated luminosity of 100 fb^{-1} , one expects 5.5×10^9 Z -bosons to be produced [10]. In particular, with the GigaZ option at the proposed International Linear Collider (ILC) with an integrated luminosity of 30 fb^{-1} , it is possible to produce more than 10^9 Z -bosons [11]. For the study of the Higgs boson, one may expect the ILC to scrutinize the Higgs-boson property after the discovery at the LHC.

These rare decays $Z \rightarrow b\bar{s}$ and $h \rightarrow b\bar{s}$ have been studied in the SM [12] and in various new physics models [13,14]. In the SM it was found that $\text{Br}(Z \rightarrow b\bar{s} + s\bar{b}) \sim 10^{-8}$ [15], and $\text{Br}(h \rightarrow b\bar{s} + s\bar{b}) \sim 10^{-7}$ (10^{-9}) for $m_h = 100 \text{ GeV}$ (200 GeV) [16]. The current sensitivity of the measurement for the branching ratios of rare Z -decays is about 10^{-5} [17]. In this work we will study these decays in the LHT model. Since such decays are strongly correlated with the induced FCNC B -decays ($B \rightarrow X_s \gamma$, $B_s \rightarrow \mu^+ \mu^-$, and $B \rightarrow X_s \mu^+ \mu^-$), we will collectively consider all these decays. We will first check the analytic results of these B -decays given in [6–9] and then perform their numerical calculations together with $Z \rightarrow b\bar{s}$ and $h \rightarrow b\bar{s}$. We will show the constraints on the parameter space from current B -decay experiments and display the results for $Z \rightarrow b\bar{s}$ and $h \rightarrow b\bar{s}$ with and without the B -decay constraints.

This work is organized as follows. In Sec. II we recapitulate the LHT model and address the new flavor-violating interactions which will contribute to the FCNC decays considered in this work. In Secs. III, IV, and V we examine the B -decays ($B \rightarrow X_s \gamma$, $B_s \rightarrow \mu^+ \mu^-$, and $B \rightarrow X_s \mu^+ \mu^-$), Z -boson decay $Z \rightarrow b\bar{s}$, and Higgs-boson decay $h \rightarrow b\bar{s}$, respectively. Finally, we give our conclusion in Sec. VI.

II. THE LITTLEST HIGGS MODEL WITH T -PARITY

The LHT model [5] is based on a nonlinear sigma model describing the spontaneous breaking of a global $SU(5)$

$$\Pi = \begin{pmatrix} -\frac{\omega^0}{2} - \frac{\eta}{\sqrt{20}} & -\frac{\omega^+}{\sqrt{2}} & -i\frac{\pi^+}{\sqrt{2}} & -i\phi^{++} & -i\frac{\phi^+}{\sqrt{2}} \\ -\frac{\omega^-}{\sqrt{2}} & \frac{\omega^0}{2} - \frac{\eta}{\sqrt{20}} & \frac{v+h+i\pi^0}{2} & -i\frac{\phi^+}{\sqrt{2}} & \frac{-i\phi^0+\phi^p}{\sqrt{2}} \\ i\frac{\pi^-}{\sqrt{2}} & \frac{v+h-i\pi^0}{2} & \sqrt{4/5}\eta & -i\frac{\pi^+}{\sqrt{2}} & \frac{v+h+i\pi^0}{2} \\ i\phi^{--} & i\frac{\phi^-}{\sqrt{2}} & i\frac{\pi^-}{\sqrt{2}} & -\frac{\omega^0}{2} - \frac{\eta}{\sqrt{20}} & -\frac{\omega^-}{\sqrt{2}} \\ i\frac{\phi^-}{\sqrt{2}} & \frac{i\phi^0+\phi^p}{\sqrt{2}} & \frac{v+h-i\pi^0}{2} & -\frac{\omega^+}{\sqrt{2}} & \frac{\omega^0}{2} - \frac{\eta}{\sqrt{20}} \end{pmatrix}. \quad (1)$$

Under T -parity the SM Higgs doublet $H = (-i\pi^+/\sqrt{2}, (v+h+i\pi^0)/2)^T$ is T -even, while the other fields are T -odd. A subgroup $[SU(2) \times U(1)]_1 \times [SU(2) \times U(1)]_2$ of the $SU(5)$ is gauged, and at the scale f it is broken into the SM electroweak symmetry $SU(2)_L \times U(1)_Y$. The Goldstone bosons ω^0 , ω^\pm , and η are, respectively, eaten by the new T -odd gauge bosons Z_H , W_H , and A_H , which obtain masses at $\mathcal{O}(v^2/f^2)$

$$M_{W_H} = M_{Z_H} = fg \left(1 - \frac{v^2}{8f^2}\right), \quad (2)$$

$$M_{A_H} = \frac{fg'}{\sqrt{5}} \left(1 - \frac{5v^2}{8f^2}\right),$$

with g and g' being the SM $SU(2)$ and $U(1)$ gauge couplings, respectively.

The Goldstone bosons π^0 and π^\pm are eaten by the SM T -even Z -boson and W -boson, which obtain masses at $\mathcal{O}(v^2/f^2)$,

$$M_{W_L} = \frac{gv}{2} \left(1 - \frac{v^2}{12f^2}\right), \quad M_{Z_L} = \frac{gv}{2 \cos\theta_W} \left(1 - \frac{v^2}{12f^2}\right). \quad (3)$$

The photon A_L is also T -even and massless. Because of the mass of SM bosons corrected at $\mathcal{O}(v^2/f^2)$, the relation between G_F and v is modified from its SM form and is given by $\frac{1}{v^2} = \sqrt{2}G_F(1 - \frac{v^2}{6f^2})$.

The top quark has a T -even partner T quark and a T -odd T_- quark. To leading order, their masses are given by

down to a global $SO(5)$ by a 5×5 symmetric tensor at the scale $f \sim \mathcal{O}(\text{TeV})$. From the $SU(5)/SO(5)$ breaking, there arise 14 Goldstone bosons which are described by the ‘‘pion’’ matrix Π , given explicitly by

$$M_T = \frac{m_t f}{v} \left(r + \frac{1}{r}\right), \quad M_{T_-} = M_T \frac{1}{\sqrt{1+r^2}}, \quad (4)$$

where $r = \lambda_1/\lambda_2$ with λ_1 and λ_2 being the coupling constants in the Lagrangian of the top quark sector [5]. Furthermore, for each SM quark (lepton), a copy of mirror quark (lepton) with T -odd quantum number is added in order to preserve the T -parity. We denote them by u_H^i , d_H^i , ν_H^i , l_H^i , where $i = 1, 2, 3$ are the generation index. In $\mathcal{O}(v^2/f^2)$ their masses satisfy

$$m_{d_H^i} = \sqrt{2}\kappa_{q^i}f, \quad m_{u_H^i} = m_{d_H^i} \left(1 - \frac{v^2}{8f^2}\right). \quad (5)$$

Here κ_{q^i} are the diagonalized Yukawa couplings of the mirror quarks.

Note that new flavor interactions arise between the mirror fermions and the SM fermions, mediated by the T -odd gauge bosons or T -odd Goldstone bosons. In general, besides the charged-current flavor-changing interactions, the FCNC interactions between the mirror fermions and the SM fermions can also arise from the mismatch of rotation matrices. For example, there exist FCNC interactions between the mirror down-type quarks and the SM down-type quarks, where the mismatched mixing matrix is denoted by V_{H_d} . We follow [18] to parametrize V_{H_d} with three angles θ_{12}^d , θ_{23}^d , θ_{13}^d and three phases δ_{12}^d , δ_{23}^d , δ_{13}^d

$$\begin{pmatrix} c_{12}^d c_{13}^d & s_{12}^d c_{13}^d e^{-i\delta_{12}^d} & s_{13}^d e^{-i\delta_{13}^d} \\ -s_{12}^d c_{23}^d e^{i\delta_{12}^d} - c_{12}^d s_{23}^d s_{13}^d e^{i(\delta_{13}^d - \delta_{23}^d)} & c_{12}^d c_{23}^d - s_{12}^d s_{23}^d s_{13}^d e^{i(\delta_{13}^d - \delta_{12}^d - \delta_{23}^d)} & s_{23}^d c_{13}^d e^{-i\delta_{23}^d} \\ s_{12}^d s_{23}^d e^{i(\delta_{12}^d + \delta_{23}^d)} - c_{12}^d c_{23}^d s_{13}^d e^{i\delta_{13}^d} & -c_{12}^d s_{23}^d e^{i\delta_{23}^d} - s_{12}^d c_{23}^d s_{13}^d e^{i(\delta_{13}^d - \delta_{12}^d)} & c_{23}^d c_{13}^d \end{pmatrix}. \quad (6)$$

III. FCNC B -DECAYS

The decays $B \rightarrow X_s \gamma$, $B_s \rightarrow \mu^+ \mu^-$, and $B \rightarrow X_s \mu^+ \mu^-$ can be induced at loop level by the new flavor-changing interactions in the LHT model and have been recently studied in [8,9]. We check the results of [8,9] and make

the following brief descriptions about these decays without giving the detailed expressions (all functions in our following discussions can be found in [8,9]).

- (1) For $B \rightarrow X_s \gamma$ the LHT contributions enter through the modifications of the quantities

$$\begin{aligned}
 T_{D'}^{\text{SM}} &\equiv \lambda_t^{(s)} D_0'(x_t) = -2\lambda_t^{(s)} C_{7\gamma}^{0\text{SM}}(M_W), \\
 T_{E'}^{\text{SM}} &\equiv \lambda_t^{(s)} E_0'(x_t) = -2\lambda_t^{(s)} C_{8G}^{0\text{SM}}(M_W),
 \end{aligned} \tag{7}$$

where the Cabibbo-Kobayashi-Maskawa (CKM) factor $\lambda_t^{(s)} = V_{ts} V_{tb}^*$, and $C_{7\gamma}^{0\text{SM}}$, and $C_{8G}^{0\text{SM}}$ are leading-order Wilson coefficients. With the LHT effects $T_{D'}^{\text{SM}}$ and $T_{E'}^{\text{SM}}$ are replaced by $T_{D'}$ and $T_{E'}$

$$T_{D'} = T_{D'}^{\text{even}} + T_{D'}^{\text{odd}}, \quad T_{E'} = T_{E'}^{\text{even}} + T_{E'}^{\text{odd}}, \tag{8}$$

where the superscripts ‘‘even’’ and ‘‘odd’’ denote the contributions from T -even and T -odd particles, respectively. Note that for the LHT contributions we only consider the leading-order effects while for the SM prediction we consider the next-to-leading-order QCD corrections. Actually, the SM prediction for $B \rightarrow X_s \gamma$ has been calculated to NNLO [19].

- (2) The branching ratio of $B_s \rightarrow \mu^+ \mu^-$ in the SM depends on a function Y_{SM} , and the LHT effects enter through the modification of Y_{SM} [8]. With the LHT effects Y_{SM} is replaced by

$$Y_s = Y_{\text{SM}} + \bar{Y}^{\text{even}} + \frac{\bar{Y}_s^{\text{odd}}}{\lambda_t^{(s)}}, \tag{9}$$

where \bar{Y}^{even} and \bar{Y}_s^{odd} represent the effects from T -even and T -odd particles, respectively. The branching ratio normalized to the SM prediction is then given by

$$\frac{\text{Br}(B_s \rightarrow \mu^+ \mu^-)}{\text{Br}(B_s \rightarrow \mu^+ \mu^-)_{\text{SM}}} = \left| \frac{Y_s}{Y_{\text{SM}}} \right|^2 \tag{10}$$

with $\text{Br}(B_s \rightarrow \mu^+ \mu^-)_{\text{SM}} = 3.66 \times 10^{-9}$.

- (3) The branching ratio of $B \rightarrow X_s \mu^+ \mu^-$ in the SM depends on the functions Y_{SM} , Z_{SM} , and $D_0'(x_t)$ (Y_{SM} and D_0' are same as in $B_s \rightarrow \mu^+ \mu^-$ and $B \rightarrow X_s \gamma$) and the LHT effects enter through the modification of these functions. The modifications of Y_{SM} and D_0' have been given above, and the modification of Z_{SM} is given by [8]

$$Z_s = Z_{\text{SM}} + \bar{Z}^{\text{even}} + \frac{\bar{Z}_s^{\text{odd}}}{\lambda_t^{(s)}}, \tag{11}$$

where \bar{Z}^{even} and \bar{Z}_s^{odd} represent the effects from T -even and T -odd particles, respectively.

- (4) The experimental values of the branching ratios of these decays modes are given by [20]

$$\text{Br}(B \rightarrow X_s \gamma) = (3.52 \pm 0.23 \pm 0.09) \times 10^{-4} \quad (E_\gamma > 1.6 \text{ GeV}),$$

$$\text{Br}(B_s \rightarrow \mu^+ \mu^-) < 7.5 \times 10^{-8},$$

$$\text{Br}(B \rightarrow X_s \mu^+ \mu^-) = 4.3_{-1.2}^{+1.3} \times 10^{-6}. \tag{12}$$

Note that throughout this work we perform our

calculations in the 't Hooft-Feynman gauge, and the SM input parameters involved are taken from [21].

IV. Z-BOSON FCNC DECAY $Z \rightarrow b\bar{s}$

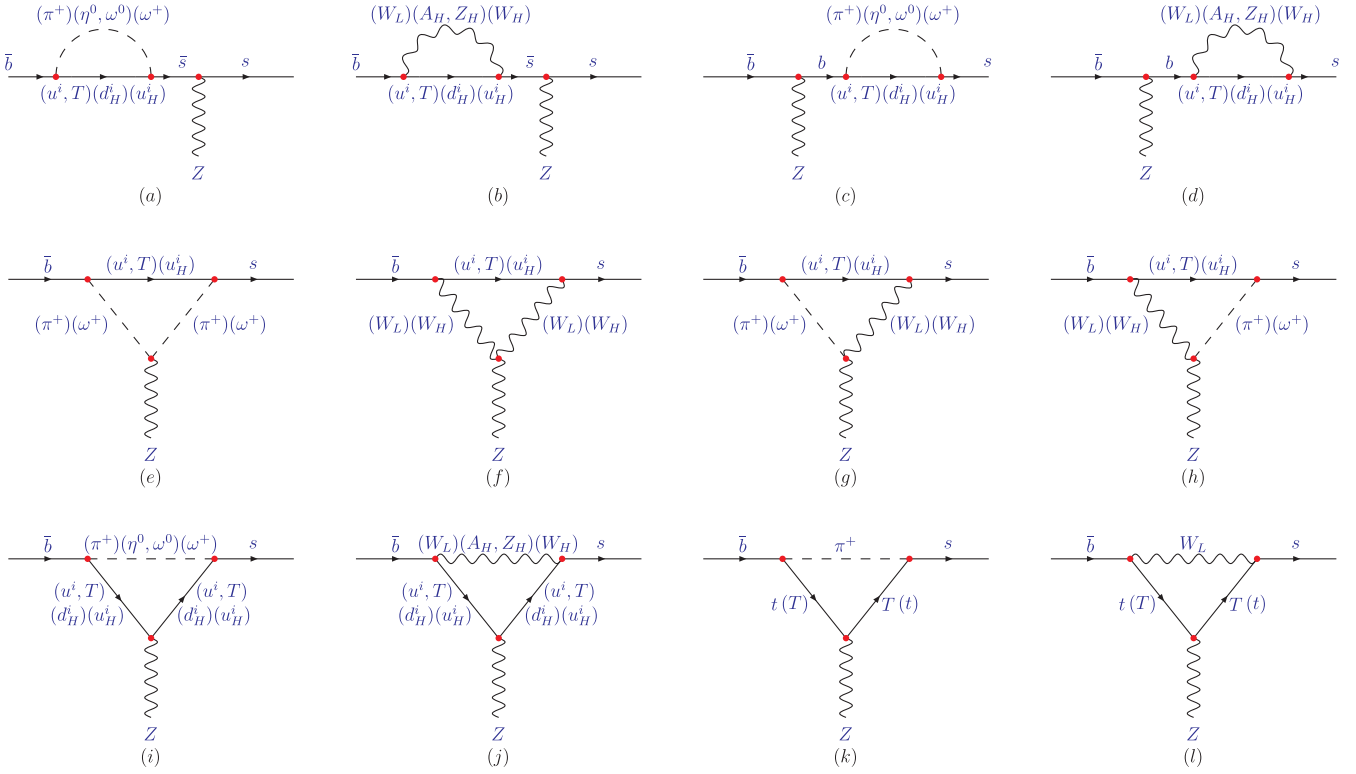
The relevant Feynman diagrams are shown in Fig. 1. The LHT contributions are from both T -even and T -odd particles. The contributions of T -even particles include both the SM contributions and the contributions of the top quark T -even partner (T -quark). The diagrams of T -odd particles are induced by the interactions between the SM quarks and the mirror quarks mediated by the heavy T -odd gauge bosons or Goldstone bosons. The calculations of the loop diagrams in Fig. 1 are straightforward. Each loop diagram is composed of some scalar loop functions [22], which are calculated by using LOOPTOOLS [23]. The relevant Feynman rules can be found in [8]. The analytic expressions from our calculation are presented in Appendix A. We have checked that the divergences of T -even contributions are cancelled at $\mathcal{O}(v^2/f^2)$. For the contributions of T -odd particles, the divergences are not cancelled at $\mathcal{O}(v^2/f^2)$ and arise from the diagrams with T -odd Goldstone bosons. Such leftover divergence in the LHT model was first found in the calculation of $B_s \rightarrow \mu^+ \mu^-$ and $B \rightarrow X_s \mu^+ \mu^-$ in [8], and was understood as the sensitivity of the decay amplitudes to the ultraviolet completion of the theory. In our numerical calculations we follow [8] to remove the divergent term $1/\epsilon$ and take the renormalization scale $\mu = \Lambda$ with $\Lambda = 4\pi f$ being the cutoff scale of the LHT model.

About the parameters f and r , some constraints come from the electroweak precision data [24], which, however, depend on the masses of T -odd fermions and the parameter δ_c (its value is related to the details of the ultraviolet completion of the theory). Hence, in our numerical calculations we relax the constraints on the parameters f and r , and let them vary in the range

$$500 \text{ GeV} \leq f \leq 1500 \text{ GeV}, \quad 0.5 \leq r \leq 2.0. \tag{13}$$

In addition to the parameters f and r , the matrix V_{Hd} and the masses of d_H^i ($i = 1, 2, 3$) are also involved in our calculations. To simplify our calculations, we follow [8] to consider three scenarios for these parameters:

- (I) We assume $V_{Hd} = 1$ or assume the degeneracy for the masses of d_H^i , i.e., $m_{d_H^1} = m_{d_H^2} = m_{d_H^3}$. In the former case, we have no flavor mixing between mirror down-type quarks and the SM down-type quarks and thus the loop contributions of T -odd particles vanish. In the latter case, due to the relation of Eq. (5), the masses of u_H^i are also degenerate. Then, due to the unitarity of the flavor-mixing matrices between mirror quarks and the SM quarks, the loop contributions of T -odd particles vanish. The remaining contributions from the loops of T -even

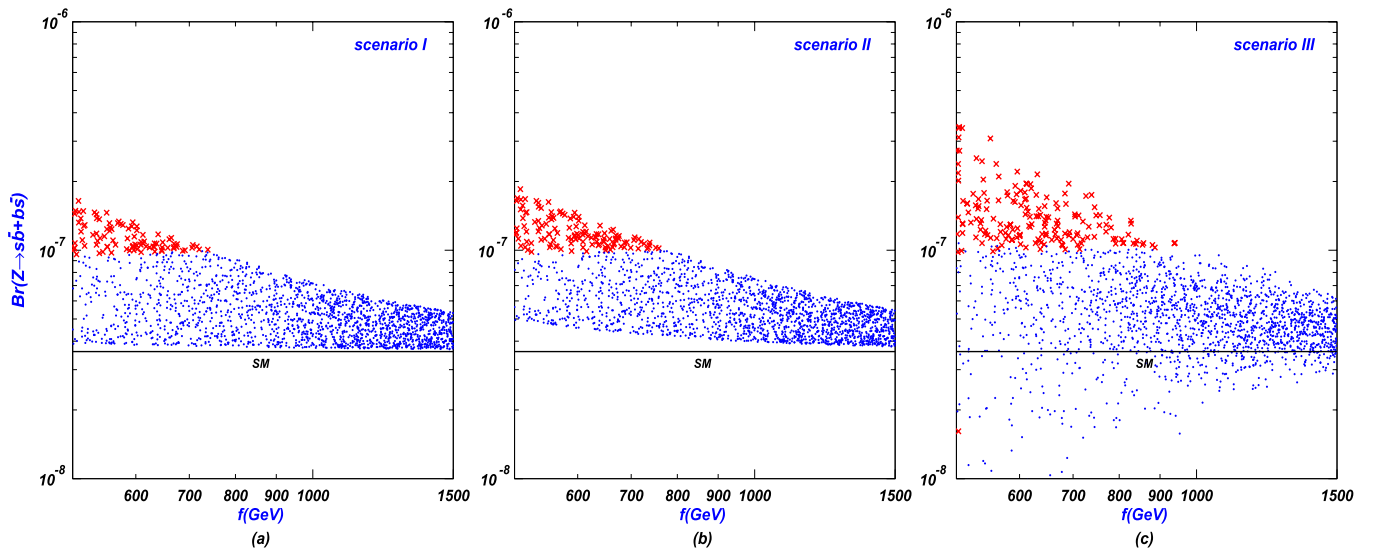

 FIG. 1 (color online). Feynman diagrams for $Z \rightarrow s\bar{b}$ in the LHT model.

particles depend on two parameters, i.e., the breaking scale f and the ratio r .

- (II) We assume $V_{Hd} = V_{\text{CKM}}$. In this scenario, in addition to the contributions of T -even particles, the T -odd particles will also come into play. The parameters involved are then f , r , $m_{d_H^i}$, and $m_{\nu_H^i}$ (the loop contributions to $B_s \rightarrow \mu^+ \mu^-$ and $B \rightarrow$

$X_s \mu^+ \mu^-$ involve the mirror lepton masses $m_{\nu_H^i}$). As shown in Eq. (5), the masses of mirror fermions are proportional to f , which are assumed as

$$\begin{aligned} m_{\nu_H^1} &= m_{\nu_H^2} = m_{\nu_H^3} = 0.5f, \\ m_{d_H^1} &= m_{d_H^2} = 0.6f, \quad m_{d_H^3} = 1.4f. \end{aligned} \quad (14)$$


 FIG. 2 (color online). Scatter plots for the branching ratio of $Z \rightarrow s\bar{b} + b\bar{s}$ versus f . The bullets (blue) and the crosses (red) are allowed and excluded by the 2σ B -decay constraints, respectively.

We checked that the parameters taken here satisfy the constraints from the four-fermion interaction operators [25].

- (III) We keep δ_{13}^d as a free parameter, while for other parameters in the matrix V_{Hd} we assume

$$\begin{aligned} \delta_{12}^d &= \delta_{23}^d = 0, \\ \frac{1}{\sqrt{2}} &\leq s_{12}^d \leq 0.99, \\ 5 \times 10^{-5} &\leq s_{23}^d \leq 2 \times 10^{-4}, \\ 4 \times 10^{-2} &\leq s_{13}^d \leq 0.6. \end{aligned} \quad (15)$$

For the masses $m_{d_H^i}$ and $m_{\nu_H^i}$, we take the same assumption as in scenario II.

We scan over the parameters in the ranges specified above. For the three scenarios we obtain the scatter plots in Fig. 2, where we also show the constraints from the B -decays $B \rightarrow X_s \gamma$, $B_s \rightarrow \mu^+ \mu^-$, and $B \rightarrow X_s \mu^+ \mu^-$.

Figure 2 shows that the contributions are sensitive to the scale f and for lower values of f the derivation from the SM prediction is more sizable. The constraints from B -decays are significant, with scenario-III being most stringently constrained.

Figure 2 also shows that for all three scenarios the branching ratio of the FCNC Z -decay is cut around 10^{-7} . The reason is that for each scenario the LHT effects in the FCNC Z -decay are strongly correlated with the effects in the FCNC B -decays. Then when the Z -decay branching ratio exceeds about 10^{-7} , the corresponding effects in B -decays go beyond the 2σ experimental region.

V. HIGGS-BOSON FCNC DECAY $h \rightarrow b\bar{s}$

The relevant Feynman diagrams involving T -even particles in the loops can be obtained from the corresponding diagrams in Fig. 1 by replacing the Z -boson with the

Higgs-boson. For the contributions of T -odd particles, the diagrams are more complicated. Note that the divergence of T -odd contributions for $h \rightarrow b\bar{s}$ is at $\mathcal{O}(1)$ and is more severe than in B -decays or Z -decay where the divergence appears at $\mathcal{O}(v^2/f^2)$. Such divergence is mainly due to the absence of Fig. 1(i) with the down-type mirror quarks in the loops since the Higgs boson does not couple to the down-type mirror quarks. Since such leftover divergences in the T -odd contributions appear at $\mathcal{O}(1)$, the prediction is subject to severe theoretical uncertainty. Unlike the uncertainty in Z -decay which is correlated with the uncertainty in B -decays (and thus can be restrained by B -decays), the uncertainty in $h \rightarrow b\bar{s}$ caused by such T -odd contributions cannot be constrained by B -decays since the contributions of the diagrams mediated by the Higgs-boson can be neglected for the B -decays. To avoid such large unconstrained uncertainty caused by T -odd contributions, we perform numerical calculations only for scenario-I where the T -odd contributions vanish. The analytic expressions for the effective coupling $hb\bar{s}$ from our calculation are presented in Appendix B.

To evaluate the branching ratio of $h \rightarrow b\bar{s}$ we need to know the total decay width of the Higgs boson. In addition to the decay channels in the SM, there arises a new important channel $h \rightarrow A_H A_H$ (A_H is a candidate for the cosmic dark matter), which may be dominant in some parameter space of the LHT model [26]. The total decay width is given by

$$\Gamma_{\text{total}} \approx \Gamma_{h \rightarrow \text{fermions}} + \Gamma_{h \rightarrow W_L W_L} + \Gamma_{h \rightarrow Z_L Z_L} + \Gamma_{h \rightarrow A_H A_H}. \quad (16)$$

In Fig. 3(a) we scan over r and f in the ranges in Eq. (13) and present the scatter plots for the branching ratio with $m_h = 140$ GeV. In Fig. 3(b) we show the dependence of the branching ratio on the Higgs-boson mass by fixing the parameters r and f allowed by the electroweak precision

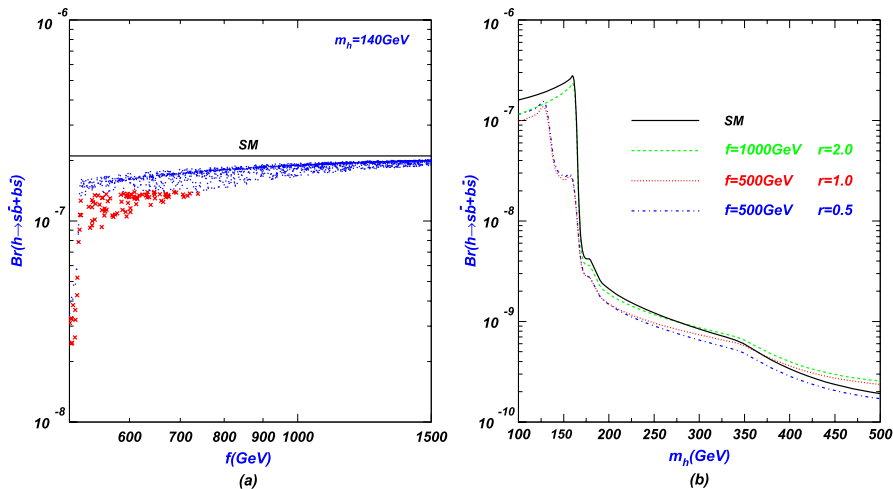


FIG. 3 (color online). (a) The scatter plots of $\text{Br}(h \rightarrow s\bar{b} + b\bar{s})$ versus f for scenario-I. The bullets (blue) and the crosses (red) are allowed and excluded by the 2σ B -decay constraints, respectively. (b) $\text{Br}(h \rightarrow s\bar{b} + b\bar{s})$ versus m_h for fixed values of f and r .

data and B -decays. In our calculations we kept the order up to $\mathcal{O}(v/f)$ and checked that the divergences are canceled to this order.

From Fig. 3 we see that the branching ratio in the LHT model is below the SM prediction and the deviation is significant for a low value of f . In the parameter space allowed by B -decays at 2σ level, the branching ratio can be one order below the SM prediction due to the fact that in some parameter space the decay $h \rightarrow A_H A_H$ may be dominant and greatly enhance the total width.

VI. CONCLUSION

The littlest Higgs model with T -parity may have a flavor problem since it predicts new flavor-changing interactions between mirror fermions and the standard model fermions, which can induce various FCNC decays. Since all the decays induced in this model are correlated, we have performed a collective study for the FCNC decays of B -mesons, the Z -boson, and the Higgs boson. We found that under the current experimental constraints from B -decays, the branching ratios of both $Z \rightarrow b\bar{s}$ and $h \rightarrow b\bar{s}$ can still deviate from the SM predictions significantly. In the parameter space allowed by B -decays, the branching ratio of $Z \rightarrow b\bar{s}$ can be enhanced up to 10^{-7} (about one order above the SM prediction) while $h \rightarrow b\bar{s}$ can be much

suppressed relative to the SM prediction (about one order below the SM prediction).

We remark that unlike the FCNC B -decays, it is quite challenging to test these rare Z -boson and Higgs-boson decays at collider experiments. For instance, to test this rare decay of the Z -boson, we may need the GigaZ option of the ILC. Theoretically, for the test of the LHT model, these rare decays are complementary to the direct production of the T -quark [27] and the production of the top quark or Higgs boson [28] whose cross sections can be sizably altered by the LHT model.

ACKNOWLEDGMENTS

This work was supported in part by National Natural Science Foundation of China (NNSFC) under Grant Nos. 10725526 and 10635030.

APPENDIX A: THE EFFECTIVE COUPLING OF $Zs\bar{b}$

Here we give the analytic expressions for the effective coupling of $Zs\bar{b}$ in the LHT model. The effective coupling of $Zb\bar{s}$ is similar and can be obtained by some simple replacements. The effective coupling of $Zs\bar{b}$ is given by

$$\begin{aligned} \Gamma_{Zs\bar{b}}^\mu = & \Gamma_{\text{self}(a)}^\mu[\pi^+, u^i(T)] + \Gamma_{\text{self}(a)}^\mu[\omega^0(\eta), d_H^i] + \Gamma_{\text{self}(a)}^\mu[\omega^+, u_H^i] + \Gamma_{\text{self}(b)}^\mu[W_L, u^i(T)] + \Gamma_{\text{self}(b)}^\mu[A_H(Z_H), d_H^i] \\ & + \Gamma_{\text{self}(b)}^\mu[W_H, u_H^i] + \Gamma_{\text{self}(c)}^\mu[\pi^+, u^i(T)] + \Gamma_{\text{self}(c)}^\mu[\omega^0(\eta), d_H^i] + \Gamma_{\text{self}(c)}^\mu[\omega^+, u_H^i] + \Gamma_{\text{self}(d)}^\mu[W_L, u^i(T)] \\ & + \Gamma_{\text{self}(d)}^\mu[A_H(Z_H), d_H^i] + \Gamma_{\text{self}(d)}^\mu[W_H, u_H^i] + \Gamma_{SF_1F_2}^\mu[\pi^+, u^i(T), u^i(T)] + \Gamma_{SF_1F_2}^\mu[\pi^+, t(T), T(t)] \\ & + \Gamma_{SF_1F_2}^\mu[\omega^0(\eta), d_H^i, d_H^i] + \Gamma_{SF_1F_2}^\mu[\omega^+, u_H^i, u_H^i] + \Gamma_{VF_1F_2}^\mu[W_L, u^i(T), u^i(T)] + \Gamma_{VF_1F_2}^\mu[W_L, t(T), T(t)] \\ & + \Gamma_{VF_1F_2}^\mu[A_H(Z_H), d_H^i, d_H^i] + \Gamma_{VF_1F_2}^\mu[W_H, u_H^i, u_H^i] + \Gamma_{FSS}^\mu[u^i(T), \pi^+, \pi^-] + \Gamma_{FSS}^\mu[u_H^i, \omega^+, \omega^-] \\ & + \Gamma_{FVV}^\mu[u^i(T), W_L, W_L] + \Gamma_{FVV}^\mu[u_H^i, W_H, W_H] + \Gamma_{FVS}^\mu[u^i(T), W_L, \pi^-] + \Gamma_{FVS}^\mu[u_H^i, W_H, \omega^-] \\ & + \Gamma_{FSV}^\mu[u^i(T), \pi^+, W_L] + \Gamma_{FSV}^\mu[u_H^i, \omega^+, W_H], \end{aligned} \quad (\text{A1})$$

where the particles in the square brackets represent the particles which contribute to the vertex. The self-energy and vertex contributions in the above equation are given by

$$\begin{aligned} \Gamma_{\text{self}(a)}^\mu = & \frac{ig}{16\pi^2 c_W (q_b^2 - m_s^2)} \gamma^\mu \left[\left(-\frac{1}{2} + \frac{1}{3} s_W^2 \right) P_L + \frac{1}{3} s_W^2 P_R \right] (\not{q}_b + m_s) [(B_\nu \gamma^\nu + \not{q}_b B_0)(a_3 b_2 P_L + a_2 b_3 P_R) \\ & + m_F B_0 (a_2 a_3 P_L + b_2 b_3 P_R)] (q_b, m_S, m_F), \end{aligned} \quad (\text{A2})$$

$$\begin{aligned} \Gamma_{\text{self}(b)}^\mu = & -\frac{ig}{16\pi^2 c_W (q_b^2 - m_s^2)} \gamma^\mu \left[\left(-\frac{1}{2} + \frac{1}{3} s_W^2 \right) P_L + \frac{1}{3} s_W^2 P_R \right] (\not{q}_b + m_s) [(2B_\nu \gamma^\nu + (2B_0 - 1)\not{q}_b)(c_2 c_3 P_L + d_2 d_3 P_R) \\ & - 2m_F (2B_0 - 1)(c_3 d_2 P_L + c_2 d_3 P_R)] (q_b, m_V, m_F), \end{aligned} \quad (\text{A3})$$

$$\begin{aligned} \Gamma_{\text{self}(c)}^\mu = & \frac{ig}{16\pi^2 c_W (p_s^2 - m_b^2)} [(B_\nu \gamma^\nu + \not{p}_s B_0)(a_3 b_2 P_L + a_2 b_3 P_R) + m_F B_0 (a_2 a_3 P_L + b_2 b_3 P_R)] \\ & \times (\not{p}_s + m_b) \gamma^\mu \left[\left(-\frac{1}{2} + \frac{1}{3} s_W^2 \right) P_L + \frac{1}{3} s_W^2 P_R \right] (p_s, m_S, m_F), \end{aligned} \quad (\text{A4})$$

$$\Gamma_{\text{self}(d)}^\mu = -\frac{ig}{16\pi^2 c_W (p_s^2 - m_b^2)} [(2B_\nu \gamma^\nu + (2B_0 - 1) \not{p}_s) (c_2 c_3 P_L + d_2 d_3 P_R) - 2m_F (2B_0 - 1) (c_3 d_2 P_L + c_2 d_3 P_R)] \\ \times (\not{p}_s + m_b) \gamma^\mu \left[\left(-\frac{1}{2} + \frac{1}{3} s_W^2 \right) P_L + \frac{1}{3} s_W^2 P_R \right] (p_s, m_V, m_F), \quad (\text{A5})$$

$$\Gamma_{SF_1 F_2}^\mu = \frac{i}{16\pi^2} \left[C_{\sigma\rho} \gamma^\sigma \gamma^\mu \gamma^\rho (a_3 b_2 Z_R^f P_L + a_2 b_3 Z_L^f P_R) + \frac{1}{2} \gamma^\mu (a_3 b_2 Z_R^f P_L + a_2 b_3 Z_L^f P_R) \right. \\ \left. + C_\nu \gamma^\nu \gamma^\mu (a_2 Z_L^f P_L + b_2 Z_R^f P_R) (\not{q}_s + \not{q}_b + m_{F_2}) (a_3 P_L + b_3 P_R) + m_{F_1} \gamma^\mu (b_2 b_3 Z_L^f P_L + a_2 a_3 Z_R^f P_R) C_\nu \gamma^\nu \right. \\ \left. + m_{F_1} \gamma^\mu (b_2 Z_L^f P_L + a_2 Z_R^f P_R) (\not{q}_s + \not{q}_b + m_{F_2}) (a_3 P_L + b_3 P_R) C_0 \right] (q_s, q_b, m_{F_1}, m_S, m_{F_2}), \quad (\text{A6})$$

$$\Gamma_{VF_1 F_2}^\mu = \frac{i}{16\pi^2} [(d_2 Z_R^f P_L + c_2 Z_L^f P_R) (-2C_{\sigma\rho} \gamma^\sigma \gamma^\mu \gamma^\rho - 2\gamma^\mu) (c_3 P_L + d_3 P_R) \\ - 2(\not{q}_s + \not{q}_b) \gamma^\mu C_\nu \gamma^\nu (c_2 c_3 Z_L^f P_L + d_2 d_3 Z_R^f P_R) + 4m_{F_2} (c_3 d_2 Z_R^f P_L + c_2 d_3 Z_L^f P_R) C_\mu \\ + 4m_{F_1} (c_3 d_2 Z_L^f P_L + c_2 d_3 Z_R^f P_R) C_\mu + 2m_{F_1} C_0 (d_2 Z_L^f P_L + c_2 Z_R^f P_R) (2(q_s + q_b)^\mu - m_{F_2} \gamma^\mu) (c_3 P_L + d_3 P_R)] \\ \times (q_s, q_b, m_{F_1}, m_V, m_{F_2}), \quad (\text{A7})$$

$$\Gamma_{FSS}^\mu = -\frac{ig_{VSS}}{16\pi^2} \{-2C_{\mu\nu} \gamma^\nu (a_3 b_2 P_L + a_2 b_3 P_R) - (q_s + q_b)^\mu C_\nu \gamma^\nu (a_3 b_2 P_L + a_2 b_3 P_R) \\ + [-2C_\mu - (q_s + q_b)^\mu C_0] \not{q}_b (a_3 b_2 P_L + a_2 b_3 P_R) + m_F [-2C_\mu - (q_s + q_b)^\mu C_0] (a_2 a_3 P_L + b_2 b_3 P_R)\} \\ \times (q_b, q_s, m_S, m_F, m_S), \quad (\text{A8})$$

$$\Gamma_{FVV}^\mu = \frac{ig_{c_W}}{16\pi^2} (d_2 P_L + c_2 P_R) \left\{ -4C_{\mu\nu} \gamma^\nu + \gamma^\mu - 2C_\nu \gamma^\nu (q_s + q_b)^\mu + 2(4m_F - 2\not{q}_b) C_\mu + (4m_F - 2\not{q}_b) (q_s + q_b)^\mu C_0 \right. \\ \left. - \left[C_{\sigma\rho} g^{\sigma\rho} - \frac{1}{2} \right] \gamma^\mu - C_\nu \gamma^\nu (\not{q}_b + m_F) \gamma^\mu - \not{p}_Z C_\nu \gamma^\nu \gamma^\mu - \not{p}_Z (\not{q}_b + m_F) \gamma^\mu C_0 - \left[C_{\sigma\rho} g^{\sigma\rho} - \frac{1}{2} \right] \gamma^\mu \right. \\ \left. + C_\nu \gamma^\nu \gamma^\mu (\not{p}_Z - \not{q}_s - \not{q}_b) - \gamma^\mu (\not{q}_b + m_F) C_\nu \gamma^\nu + \gamma^\mu (\not{q}_b + m_F) (\not{p}_Z - \not{q}_s - \not{q}_b) C_0 \right\} \\ \times (c_3 P_L + d_3 P_R) (q_b, q_s, m_V, m_F, m_V), \quad (\text{A9})$$

$$\Gamma_{FVS}^\mu = -\frac{ig_{VVS}}{16\pi^2} \gamma^\mu (c_2 P_L + d_2 P_R) [C_\nu \gamma^\nu + (\not{q}_b + m_F) C_0] (a_3 P_L + b_3 P_R) (q_b, q_s, m_S, m_F, m_V), \quad (\text{A10})$$

$$\Gamma_{FSV}^\mu = \frac{ig_{VVS}}{16\pi^2} (a_2 P_L + b_2 P_R) [C_\nu \gamma^\nu + (\not{q}_b + m_F) C_0] \gamma^\mu (c_3 P_L + d_3 P_R) (q_b, q_s, m_V, m_F, m_S), \quad (\text{A11})$$

where $q_b = -p_b$, $q_s = -p_s$, and $P_{L,R} = (1 \mp \gamma_5)/2$. The functions B and C are 2- and 3-point Feynman integrals [22], and their functional dependences are indicated in the brackets following them. The tensor loop functions can be expanded as the scalar functions [22]. In our calculation the contraction of Lorentz indices is performed numerically. The parameters appearing above are from

$$V\bar{s}f: i\gamma^\mu (c_2 P_L + d_2 P_R), \quad V\bar{f}b: i\gamma^\mu (c_3 P_L + d_3 P_R), \\ S\bar{s}f: a_2 P_L + b_2 P_R, \quad S\bar{f}b: a_3 P_L + b_3 P_R, \\ ZS^+ S^-: ig_{VSS} (p_{S^+}^\mu - p_{S^-}^\mu), \quad ZV^+ S^-: g_{VVS} g^{\mu\nu}, \\ Z\bar{f}_1 f_2: i\gamma^\mu (Z_L^f P_L + Z_R^f P_R),$$

where V represents gauge bosons and S represents scalar particles. These couplings represent the seven different classes of vertices involved in our calculation. In each class of vertices, the parameters a_2 , b_2 , a_3 , b_3 , c_2 , d_2 , c_3 , d_3 , g_{VSS} , g_{VVS} , Z_L^f , and Z_R^f take different values for different concrete coupling. The analytic expressions of these parameters are complicated at $\mathcal{O}(v^2/f^2)$ and can be found in [8].

APPENDIX B: THE EFFECTIVE COUPLING OF $hs\bar{b}$

We give the analytic expressions for the effective coupling of $hs\bar{b}$. The effective coupling of $hb\bar{s}$ is similar and

can be obtained by some simple replacements. The effective coupling of $hs\bar{b}$ is given by

$$\begin{aligned}\Gamma_{hs\bar{b}} = & \Gamma_{\text{self}(a)}[\pi^+, u^i(T)] + \Gamma_{\text{self}(b)}[W_L, u^i(T)] + \Gamma_{\text{self}(c)}[\pi^+, u^i(T)] + \Gamma_{\text{self}(d)}[W_L, u^i(T)] + \Gamma_{SF_1F_2}[\pi^+, u^i(T), u^i(T)] \\ & + \Gamma_{SF_1F_2}[\pi^+, t(T), T(t)] + \Gamma_{VF_1F_2}[W_L, u^i(T), u^i(T)] + \Gamma_{VF_1F_2}[W_L, t(T), T(t)] + \Gamma_{FSS}[u^i(T), \pi^+, \pi^-] \\ & + \Gamma_{FVV}[u^i(T), W_L, W_L] + \Gamma_{FVS}[u^i(T), W_L, \pi^-] + \Gamma_{FSV}[u^i(T), \pi^+, W_L],\end{aligned}\quad (\text{B1})$$

where

$$\Gamma_{\text{self}(a)} = -\frac{im_s}{16\pi^2 v(q_b^2 - m_s^2)}(\not{q}_b + m_s)[(B_\nu \gamma^\nu + \not{q}_b B_0)(a_3 b_2 P_L + a_2 b_3 P_R) + m_F B_0(a_2 a_3 P_L + b_2 b_3 P_R)](q_b, m_s, m_F),\quad (\text{B2})$$

$$\begin{aligned}\Gamma_{\text{self}(b)} = & \frac{im_s}{16\pi^2 v(q_b^2 - m_s^2)}(\not{q}_b + m_s)[(2B_\nu \gamma^\nu + (2B_0 - 1)\not{q}_b)(c_2 c_3 P_L + d_2 d_3 P_R) - 2m_F(2B_0 - 1)(c_3 d_2 P_L + c_2 d_3 P_R)] \\ & \times (q_b, m_V, m_F),\end{aligned}\quad (\text{B3})$$

$$\Gamma_{\text{self}(c)} = -\frac{im_b}{16\pi^2 v(p_s^2 - m_b^2)}[(B_\nu \gamma^\nu + \not{p}_s B_0)(a_3 b_2 P_L + a_2 b_3 P_R) + m_F B_0(a_2 a_3 P_L + b_2 b_3 P_R)](\not{p}_s + m_b)(p_s, m_s, m_F),\quad (\text{B4})$$

$$\begin{aligned}\Gamma_{\text{self}(d)} = & \frac{im_b}{16\pi^2 v(p_s^2 - m_b^2)}[(2B_\nu \gamma^\nu + (2B_0 - 1)\not{p}_s)(c_2 c_3 P_L + d_2 d_3 P_R) - 2m_F(2B_0 - 1)(c_3 d_2 P_L + c_2 d_3 P_R)] \\ & \times (\not{p}_s + m_b)(p_s, m_V, m_F),\end{aligned}\quad (\text{B5})$$

$$\begin{aligned}\Gamma_{SF_1F_2} = & \frac{i}{16\pi^2}(a_2 P_L + b_2 P_R)\left\{m_{F_1}[(g_L^f P_L + g_R^f P_R)(\not{q}_b + \not{q}_s + m_{F_2})C_0 + (g_L^f P_L + g_R^f P_R)C_\mu \gamma^\mu] \right. \\ & \left. + \left[(g_R^f P_L + g_L^f P_R)C_\mu \gamma^\mu(\not{q}_b + \not{q}_s + m_{F_2}) + (g_R^f P_L + g_L^f P_R)\left(C_{\mu\nu} g^{\mu\nu} - \frac{1}{2}\right)\right]\right\} \\ & \times (a_3 P_L + b_3 P_R)(q_s, q_b, m_{F_1}, m_s, m_{F_2}),\end{aligned}\quad (\text{B6})$$

$$\begin{aligned}\Gamma_{VF_1F_2} = & \frac{i}{16\pi^2}(d_2 P_L + c_2 P_R)\{(g_L^f P_L + g_R^f P_R)[4C_\mu(q_b + q_s)^\mu + 4C_{\mu\nu}\gamma^{\mu\nu} - 4 - 2m_{F_2}C_\mu \gamma^\mu] \\ & + (g_R^f P_L + g_L^f P_R)[2m_{F_1}(2m_{F_2} - \not{q}_b - \not{q}_s)C_0 - 2m_{F_1}C_\mu \gamma^\mu]\}(c_3 P_L + d_3 P_R)(q_s, q_b, m_{F_1}, m_V, m_{F_2}),\end{aligned}\quad (\text{B7})$$

$$\Gamma_{FSS} = -\frac{im_h^2}{16\pi^2 v}(a_2 P_L + b_2 P_R)[(\not{q}_b + m_F)C_0 + C_\mu \gamma^\mu](a_3 P_L + b_3 P_R)(q_b, q_s, m_s, m_F, m_S),\quad (\text{B8})$$

$$\Gamma_{FVV} = \frac{ig^2 v}{16\pi^2}(d_2 P_L + c_2 P_R)[(\not{q}_b - 2m_F)C_0 + C_\mu \gamma^\mu](c_3 P_L + d_3 P_R)(q_b, q_s, m_V, m_F, m_V),\quad (\text{B9})$$

$$\begin{aligned}\Gamma_{FVS} = & \frac{ig}{32\pi^2}(d_2 P_L + c_2 P_R)\left[\not{p}_h(\not{q}_b + m_F)C_0 + \not{p}_h C_\mu \gamma^\mu + C_\mu \gamma^\mu(\not{q}_b + m_F) + \left(C_{\mu\nu} g^{\mu\nu} - \frac{1}{2}\right)\right] \\ & \times (a_3 P_L + b_3 P_R)(q_b, q_s, m_s, m_F, m_V),\end{aligned}\quad (\text{B10})$$

$$\Gamma_{FSV} = \frac{ig}{32\pi^2} (a_2 P_L + b_2 P_R) \left[C_\mu \gamma^\mu (\not{p}_h - \not{q}_b - \not{q}_s) - (\not{q}_b + m_F) C_\mu \gamma^\mu - \left(C_{\mu\nu} g^{\mu\nu} - \frac{1}{2} \right) + (\not{q}_b + m_F) (\not{p}_h - \not{q}_b - \not{q}_s) C_0 \right] (c_3 P_L + d_3 P_R) (q_b, q_s, m_V, m_F, m_S). \quad (\text{B11})$$

The parameters g_L^f and g_R^f are from the couplings

$$h\bar{f}_1 f_2: i(g_L^f P_L + g_R^f P_R),$$

where

$$\begin{aligned} g_L^f &= -\frac{m_{u^i}}{v}, & g_R^f &= -\frac{m_{u^i}}{v} & (\text{for } f_1 = u_i, f_2 = u_i); \\ g_L^f &= \frac{m_t}{v} \frac{r}{1+r^2} \frac{v}{f}, & g_R^f &= \frac{m_t}{v} \frac{r}{1+r^2} \frac{v}{f} & (\text{for } f_1 = T, f_2 = T); \\ g_L^f &= \frac{m_t}{v} \frac{r}{1+r^2} \frac{v}{f}, & g_R^f &= -\frac{m_t}{v} r & (\text{for } f_1 = t, f_2 = T); \\ g_L^f &= -\frac{m_t}{v} r, & g_R^f &= \frac{m_t}{v} \frac{r}{1+r^2} \frac{v}{f} & (\text{for } f_1 = T, f_2 = t). \end{aligned}$$

-
- [1] N. Arkani-Hamed, A.G. Cohen, and H. Georgi, Phys. Lett. B **513**, 232 (2001); N. Arkani-Hamed *et al.*, J. High Energy Phys. 08 (2002) 020; 08 (2002) 021; I. Low, W. Skiba, and D. Smith, Phys. Rev. D **66**, 072001 (2002); D.E. Kaplan and M. Schmaltz, J. High Energy Phys. 10 (2003) 039.
- [2] N. Arkani-Hamed, A.G. Cohen, E. Katz, and A.E. Nelson, J. High Energy Phys. 07 (2002) 034; S. Chang, J. High Energy Phys. 12 (2003) 057; T. Han, H.E. Logan, B. McElrath, and L.T. Wang, Phys. Rev. D **67**, 095004 (2003); M. Schmaltz and D. Tucker-Smith, Annu. Rev. Nucl. Part. Sci. **55**, 229 (2005).
- [3] C. Csaki, *et al.*, Phys. Rev. D **67**, 115002 (2003); **68**, 035009 (2003); J.L. Hewett, F.J. Petriello, and T.G. Rizzo, J. High Energy Phys. 10 (2003) 062; M.C. Chen and S. Dawson, Phys. Rev. D **70**, 015003 (2004); M.C. Chen, *et al.*, Mod. Phys. Lett. A **21**, 621 (2006); W. Kilian and J. Reuter, Phys. Rev. D **70**, 015004 (2004).
- [4] G. Marandella, C. Schappacher, and A. Strumia, Phys. Rev. D **72**, 035014 (2005).
- [5] H.C. Cheng and I. Low, J. High Energy Phys. 09 (2003) 051; 08 (2004) 061; I. Low, J. High Energy Phys. 10 (2004) 067; J. Hubisz and P. Meade, Phys. Rev. D **71**, 035016 (2005).
- [6] J. Hubisz, S.J. Lee, and G. Paz, J. High Energy Phys. 06 (2006) 041.
- [7] M. Blanke *et al.*, arXiv:0805.4393.
- [8] M. Blanke *et al.*, J. High Energy Phys. 01 (2007) 066.
- [9] M. Blanke *et al.*, J. High Energy Phys. 12 (2006) 003.
- [10] A.D. Martin *et al.*, Eur. Phys. J. C **14**, 133 (2000).
- [11] J.A. Aguilar-Saavedra *et al.*, arXiv:hep-ph/0106315.
- [12] G. Eilam, Nucl. Phys. B, Proc. Suppl. **116**, 306 (2003).
- [13] C. Busch, Nucl. Phys. **B319**, 15 (1989); W.S. Hou and R.G. Stuart, Phys. Lett. B **226**, 122 (1989); B. Grzadkowski, J.F. Gunion, and P. Krawczyk, Phys. Lett. B **268**, 106 (1991); B. Mukhopadhyaya and A. Raychaudhuri, Phys. Rev. D **39**, 280 (1989); M.J. Duncan, Phys. Rev. D **31**, 1139 (1985); F. Gabbiani, J.H. Kim, and A. Masiero, Phys. Lett. B **214**, 398 (1988); M. Chemtob and G. Moreau, Phys. Rev. D **59**, 116012 (1999); W. Buchm and M. Gronau, Phys. Lett. B **220**, 641 (1989); G.T. Park and T.K. Kuo, Phys. Rev. D **42**, 3879 (1990); M.A. Perez and M.A. Soriano, Phys. Rev. D **46**, 284 (1992); J. Roldan, F.J. Botella, and J. Vidal, Phys. Lett. B **283**, 389 (1992); X.L. Wang, G.R. Lu, and Z.J. Xiao, Phys. Rev. D **51**, 4992 (1995); C.X. Yue, H. Li, and H. Zong, Nucl. Phys. **B650**, 290 (2003); R. Mohanta, Phys. Rev. D **71**, 114013 (2005).
- [14] T. Hahna *et al.*, arXiv:hep-ph/0512315; A. Arhrib *et al.*, Phys. Lett. B **647**, 36 (2007); **612**, 263 (2005); A.M. Curiel *et al.*, Phys. Rev. D **69**, 075009 (2004); A.M. Curiel, M.J. Herrero, and D. Temes, Phys. Rev. D **67**, 075008 (2003); D.A. Demir, Phys. Lett. B **571**, 193 (2003); F. Dilme *et al.*, J. High Energy Phys. 08 (2004) 018; J. Guasch *et al.*, Nucl. Phys. **B562**, 3 (1999).
- [15] M. Clements *et al.*, Phys. Rev. D **27**, 570 (1983); V. Ganapathi *et al.*, Phys. Rev. D **27**, 579 (1983); W.S. Hou *et al.*, Phys. Rev. Lett. **57**, 1406 (1986); J. Bernabeni *et al.*, Phys. Rev. Lett. **57**, 1514 (1986).
- [16] A. Arhrib, Phys. Lett. B **612**, 263 (2005); S. Bejar *et al.*, J. High Energy Phys. 08 (2004) 018; , Nucl. Phys. **B675**, 270 (2003).
- [17] S. Eidelman (Particle Data Group), Phys. Lett. B **592**, 1 (2004).
- [18] M. Blanke *et al.*, Phys. Lett. B **646**, 253 (2007).

- [19] M. Misiak *et al.*, Phys. Rev. Lett. **98**, 022002 (2007); T. Becher and M. Neubert, Phys. Rev. Lett. **98**, 022003 (2007).
- [20] The Heavy Flavor Averaging Group (HFAG), <http://www.slac.stanford.edu/xorg/hfag/>.
- [21] W.M. Yao *et al.* (Particle Data Group), J. Phys. G **33**, 1 (2006).
- [22] G. 't Hooft and M.J.G. Veltman, Nucl. Phys. **B153**, 365 (1979).
- [23] T. Hahn and M. Perez-Victoria, Comput. Phys. Commun. **118**, 153 (1999); T. Hahn, Nucl. Phys. B, Proc. Suppl. **135**, 333 (2004).
- [24] J. Hubisz, P. Meade, A. Noble, and M. Perelstein, J. High Energy Phys. 01 (2006) 135.
- [25] Q.H. Cao and C.R. Chen, Phys. Rev. D **76**, 075007 (2007).
- [26] R. S. Hundi, B. Mukhopadhyaya, and A. Nyffeler, Phys. Lett. B **649**, 280 (2007); C.R. Chen, K. Tobe, and C.P. Yuan, Phys. Lett. B **640**, 263 (2006).
- [27] K. Cheung, C. S. Kim, K. Y. Lee, and J. Song, Phys. Rev. D **74**, 115013 (2006); T. Han, R. Mahbubani, D. G. E. Walker, and L.-T. Wang, arXiv:0803.3820; S. Matsumoto, T. Moroi, and K. Tobe, Phys. Rev. D **78**, 055018 (2008).
- [28] C. O. Dib, R. Rosenfeld, and A. Zerwekh, J. High Energy Phys. 05 (2006) 074; L. Wang *et al.*, Phys. Rev. D **75**, 074006 (2007); **76**, 017702 (2007); **77**, 015020 (2008).